

Aortic Coarctation Alters Thoracic Aortic Hemodynamics Across a Large Age Range

Bradley D Allen¹, Alex J Barker¹, Julio Garcia¹, Maya Gabbour², Miachael Markl^{1,3}, Cynthia K Rigby^{1,2}, and Joshua D Robinson^{4,5}

¹Department of Radiology, Northwestern University, Chicago, IL, United States, ²Department of Medical Imaging, Ann & Robert H Lurie Children's Hospital of Chicago, Chicago, IL, United States, ³Department of Biomedical Engineering, Northwestern University, Chicago, IL, United States, ⁴Department of Pediatrics, Northwestern University, Chicago, IL, United States, ⁵Department of Cardiology, Ann & Robert H Lurie Children's Hospital of Chicago, Chicago, IL, United States

Introduction: Coarctation of the aorta is a congenital cardiovascular malformation with a prevalence of 6% in the general population, with patients exhibiting a co-morbid bicuspid aortic valve (BAV) in 40-60% of these cases.^{1,2} Conversely, patients with BAV are found to have aortic coarctation in 50-80% of cases.³ In the combined cohort, patients with both BAV and aortic coarctation are at an increased risk of aortic dissection, and are also at increased risk of restenosis following coarctation repair.^{2,4} Multiple studies have shown the presence of altered aortic hemodynamic parameters such as aortic wall shear stress throughout the thoracic aorta in this group of patients.^{2,5,6} However, it is uncertain how the changes in aortic hemodynamics associated with coarctation in combination with other abnormalities such as BAV ultimately influence disease progression.

Time-resolved 3D phase contrast (4D flow) MRI has been used previously to study patients with both BAV and aortic coarctation.² The technique is particularly well suited for this application because of the ability to visualize and quantify blood flow characteristics in an entire volume of interest.⁷ The aim of the current study is to assess the impact of aortic coarctation on aortic 3D blood flow characteristics in a cohort of pediatric, young adult, and adult patients compared to a control group without coarctation, as matched for age, valve morphology and aortic diameter.

Methods: In accordance with a local IRB-approved protocol, 19 patients with aortic coarctation (age = 27±12 years, range: 4 to 50 years) who underwent cardiovascular MRI including 4D flow MRI were retrospectively selected for inclusion in the study. Of this group, 16 patients had BAV, while 3 patients had tricuspid aortic valve (TAV). Additionally, 14 patients in this group had undergone coarctation repair, while 5 patients had not had coarctation repair. An additional 20 patients without coarctation (age = 27 ± 9 years, range: 4.0 to 64 years) who had undergone 4D flow MRI were selected as matched controls with an attempt to minimize differences in age, aortic diameter, valve morphology, aortic stenosis, and aortic regurgitation. The control group had 17 patients with BAV and 3 patients with TAV. All measurements were performed on 1.5T MR systems (Avanto, Aera, Siemens, Germany). ECG and respiratory gated 4D flow MRI was acquired in a 3D volume covering the entire thoracic aorta (spatial resolution = (2.88-3.04 x 2.13-2.31 x 2.50-3.00) mm³, temporal resolution = 37.6-39.2 ms, venc = 150-300 cm/s). Subsequent 3D blood flow visualization and quantification was performed using dedicated software (EnSight, CEI, Apex, NC). Assessment of flow jet pattern and helicity was performed in the ascending aorta, aortic arch, and descending aorta by two different observers. Aortic root and ascending aorta (AAo) diameters were indexed by body surface area of patients. Systolic flow uniformity was evaluated by identifying quadrants with systolic peak velocities >1m/s in analysis planes in the AAo, arch, and DAo. Presence and extent of helix flow was graded based on the rotation angle (N/A = 0, <180° = 1, 180°-360° = 2, 360°-540° = 3, 540°-720° = 4, >720° = 5). Helicity and flow jet pattern measurements were averaged between the two observers, and results were compared using a Wilcoxon rank-sum test. All other data was compared using a Student's t-test. The same analysis was performed to compare the subgroups of coarctation patients who had undergone repair to those who had not undergone coarctation repair.

Results: 3D visualization of systolic flow characteristics clearly illustrates enhanced flow derangement up- and downstream from the aortic pathology in a patient with coarctation (Figure 1A and 1B) compared to a control patient (Figure 1C and 1D). In comparing the coarctation to no coarctation groups (Table 1), there was no significant difference in age (p = 0.935), indexed aortic root diameter (2.09 ± 0.40 vs. 2.14 ± 0.59 cm/m², p = 0.775), or AAo diameter (1.87 ± 0.46 vs. 1.86 ± 0.75 cm/m², p = 0.942). The coarctation group had higher helicity gradings in all aortic segments (AAo: 2.05 ± 0.67 vs. 1.85 ± 0.71, p < 0.001; Arch: 1.74 ± 0.49 vs. 1.85 ± 0.40, p < 0.001; Descending Ao: 1.37 ± 0.60 vs. 0.93 ± 0.40, p < 0.001). Flow jet patterns (Figure 2) demonstrated enhanced flow eccentricity with systolic flow directed posteriorly in the AAo in both groups and high velocity flow in cranial quadrants of the arch in the coarctation group. In subgroup analysis, the coarctation group had larger indexed AAo diameters when compared to the coarctation repair group (2.29 ± 0.62 vs. 1.71 ± 0.27, p = 0.014), as well as higher grade helical flow at all three ROIs along the aorta (AAo: 2.50 ± 0.457 vs. 1.89 ± 0.66, p < 0.001; Arch: 1.40 ± 0.66 vs. 1.32 ± 0.41, p = 0.002; Descending Ao: 1.60 ± 0.49 vs. 1.29 ± 0.62, p < 0.001). There was no significant correlation between helicity grade and age for the coarct group (r = 0.35) or non-coarct group (r = -0.07), but a stronger correlation for the non-repaired coarctation subgroup (r = 0.87).

Discussion: This study demonstrates that the presence of coarctation or coarctation repair alters blood flow hemodynamics along the entire thoracic aorta in patients with both BAV and TAV in a large age range. It is notable that the coarctation group, comprised of both repaired and non-repaired coarctation patients, had significantly higher helical grade relative to the control group. This finding suggests that there is either some intrinsic difference in the aorta that alters flow regardless of repair, or that current surgical repairs do not adequately create aortic geometry that approaches the conditions in a non-diseased aorta. Additionally, the finding that there was a higher helical grade along the aorta in the subgroup of patients with coarctation, compared to repaired coarctation, demonstrates that aortic geometry and/or elasticity is linked with changes in flow patterns. Finally, the fact that there was minimal correlation with helical grade with increasing age except in the non-repaired coarctation group suggests that the hemodynamic alterations found in these patients are primarily dependent on intrinsic features of the aorta and aortic anatomy rather than age-related vascular changes.

Acknowledgements: Grant support by NIH R01 HL115828, NMH Excellence in Academic Medicine (EAM) Program 'Advanced Cardiovascular MRI Research Center', NUCATS NIH UL1RR025741 and Northwestern Memorial Foundation Dixon Translational Research Grants Initiative

References: 1. Abbruzzese PA, Aidala E. *J Cardiovasc Med.* 2007;8(2):123-122. Frydrychowicz A, et al. *Investigative radiology.* 2011;46(5):317-325. 3. Cripe L, et al. *JACC.* 2004;44(1):138-143. 4. Oliver JM, et al. *JACC.* 2004;44(8):1641-1647. 5. Oliver JM, et al. *Am. J. Card.* 2009;104(7):1001-1006. 6. Barker AJ, et al. *Circ Card Img.* 2012;5(4):457-466. 7. Markl M, et al. *JCMR.* 2011;13:7

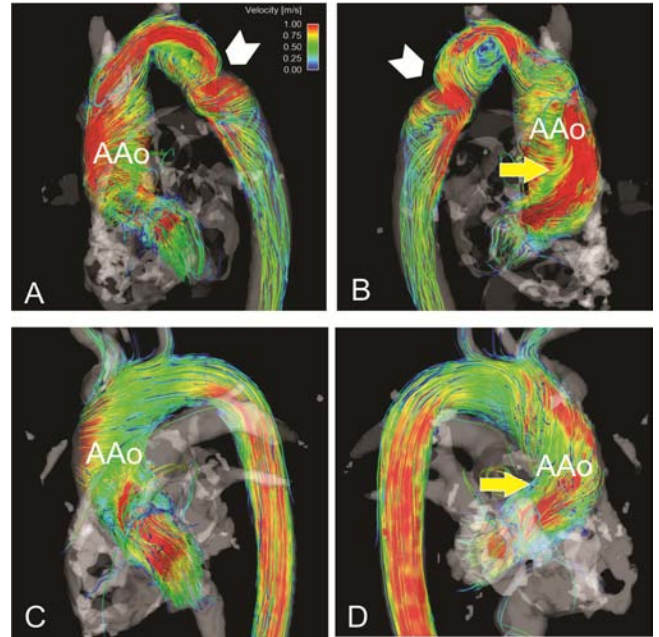


Figure 1: Velocity 3D streamline representation of blood flow. A: LAO view of coarctation patient. B: Right-posterior view of coarctation patient. Note the high velocity and high grade helical flows at coarctation (white arrowhead) C: LAO view of non-coarctation patient. D: Right-posterior view of non-coarctation patient. Note the posteriorly directed high velocity jet in the ascending aorta (AAo) in both patients, consistent with flow patterns observed in BAV patients.

	Coarct (n = 19, 16 BAV and 3 TAV)		No Coarct (n = 20, 17 BAV and 3 TAV)		P-value
	Ave	St. Dev	Ave	St. Dev	
Age	26.95	12.32	26.52	18.87	0.935
Indexed Aortic Root (cm/m ²)	2.09	0.40	2.14	0.59	0.775
Indexed Proximal AAo (cm/m ²)	1.87	0.46	1.86	0.75	0.942
Root Peak Velocity (m/s)	1.90	0.70	1.59	0.48	0.129
Root RF (%)	13.59	43.67	12.22	23.29	0.906
Mid AAo Peak Velocity (m/s)	1.66	0.65	1.68	0.68	0.930
Mid AAo RF (%)	2.81	2.98	5.78	7.06	0.107
Arch Peak Velocity (m/s)	1.60	0.55	1.35	0.54	0.176
Arch RF (%)	1.74	2.44	6.69	6.83	0.006
Descending Peak Velocity (m/s)	1.47	0.61	1.19	0.30	0.076
Descending RF (%)	2.65	3.71	6.62	7.08	0.041
AAo Helical Grade	2.05	0.67	1.85	0.71	<0.001
Arch Helical Grade	1.34	0.49	1.23	0.40	<0.001
Descending Ao Helical Grade	1.37	0.60	0.93	0.40	<0.001

Table 1: Comparison between patients with and without aortic coarctation

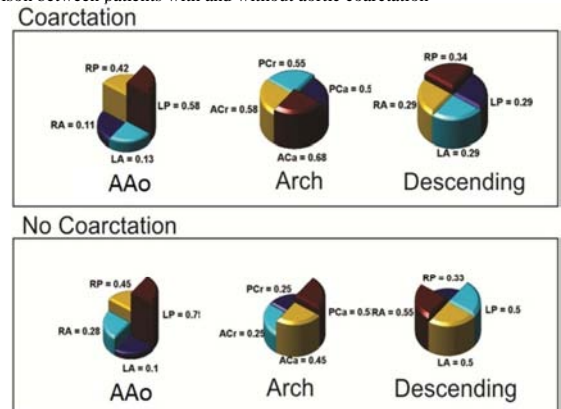


Figure 2: Flow jet profile averages for coarctation and non-coarctation group. The individual pie charts represent the number of segments (fraction of patients per group) in each group with peak velocity >1m/s. (RA – right anterior, LA – left anterior, RP – right posterior, LP – left posterior, ACr – anterior cranial, PCr – posterior cranial, ACA – anterior caudal, PCA – posterior caudal)